

Photoluminescence of Quantum Dots

Michael Schmid* and Henri Menke†

Gruppe M25, Fortgeschrittenenpraktikum, University of Stuttgart

(July 07, 2015)

Quantum dots are artificially produced structures which confine electrons and holes in a small volume in the magnitude of the de Broglie wavelength. Therefore quantum effects in form of a discrete energy spectrum arise and provide superior new applications, e.g. single photon light sources, lasers, etc. In this experiment the spectral properties of semiconductor quantum dots are investigated. At low temperatures the photoluminescence spectra of two different kind of quantum dots are measured for different laser intensities. Additionally, the spectra are also measured by varying the temperature.

BASICS

In low-dimensional systems the extent is confined in either one, two, or three orthogonal directions. We distinguish three groups of structures. A system confined in only one dimension is called a quantum film (2D structure). These are for example semiconductor heterostructures, such as AlGaAs/GaAs/AlGaAs, or graphene. If the system is confined in two dimensions we obtain a quantum wire (1D structure). If we confine all three dimensions, in the magnitude of the de Broglie wavelength, quantum effects arise. This object is then called *quantum dot*. These zero-dimensional systems are synthesised either chemically or self-organised.

There are two approaches to the production of quantum dots. Within the *top-down-approach* we start from large structures, which are treated with lithographic and etching techniques to form structures on the nano scale. Structural sizes of down to 50 nm to 30 nm are possible. Within the *bottom-up-approach* growth and self-organisation are exploited to form nano structures from atomic or molecular components. Structural sizes under 50 nm can be reached [1].

Reduction of the dimension inevitably leads to a change of physical properties of the system, including optical, magnetic, electric, and thermal properties.

According to Heisenberg's uncertainty relation one has

$$\Delta p_x \approx \frac{\hbar}{\Delta x}. \quad (1)$$

A confinement in x -direction provides the particle with an additional energy given by

$$E_{\text{Confinement}} = \frac{(\Delta p_x)^2}{2m} \approx \frac{\hbar^2}{2m(\Delta x)^2}. \quad (2)$$

This confinement energy is relevant as soon as it grows as large as the kinetic energy of the particle originating from its thermal motion in the confined direction.

Eigenstates of Quantum Dots

To calculate the electron and hole states in the zero dimensional potential of the quantum dot we assume that:

- The ratio between height and lateral extension is about 2 nm/40 nm. Due to the small extension in z -direction we can assume a potential which contains just one state. Hence in lateral direction quantum dots are, in a rough approximation, two dimensional objects.
- The potential in the x and y -directions has the form of a parabola. This assumption fits to their lensoid shape originating from the specific growth technique.
- There is no interaction between quantum dots because of their spacial distance. By typical densities of $1 \cdot 10^9 \text{ cm}^{-3}$ the average distance between each quantum dot is about 100 nm [2].

With these assumptions the eigenstates of quantum dots can be calculated with a two dimensional harmonic oscillator model or—if we assume walls instead a parabolic potential in the xy -direction—with a simple well potential. We first want to proceed with the harmonic oscillator model.

Harmonic Oscillator Model: Using the assumptions above allows us to separate the wave function in z -direction from the x and y -direction. We then can write the Hamiltonian in the form

$$\mathcal{H} = \frac{p_x^2}{2m^*} + \frac{p_y^2}{2m^*} + \frac{1}{2}m^*\omega^2 x^2 + \frac{1}{2}m^*\omega^2 y^2, \quad (3)$$

which is a *two dimensional harmonic oscillator*. Here m^* denotes the effective mass of an electron in a solid. A short calculation, known from the quantum mechanics lecture, shows that the eigenenergies are

$$E_{x,y} = \hbar\omega (n_x + n_y + 1), \quad (4)$$

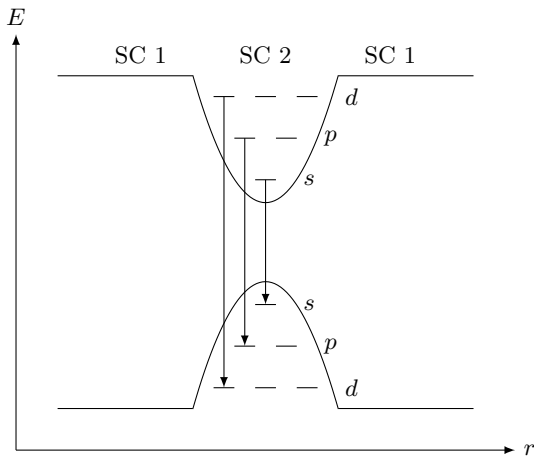


FIG. 1. Allowed transitions in a quantum dot. As depicted the abbreviation SC means semi conductor and shows that quantum dot and substrate consists of different materials.

with $n_\alpha \in \mathbb{N}_0$. The corresponding wave functions then take on the form

$$\psi_{n_x, n_y}(x, y) = \frac{\kappa}{\sqrt{2^{n_x+n_y} \pi n_x! n_y!}} e^{-\frac{\kappa}{2}(x^2+y^2)} \times H_{n_x}(\kappa x) H_{n_y}(\kappa y), \quad (5)$$

where $H_\alpha(\bullet)$ are the Hermite polynomials and κ is an effective length of electrons or holes (Calculation from [3]). For the s -state of an electron we get

$$\psi_{0,0} = \frac{\kappa_e}{\sqrt{\pi}} e^{-\frac{\kappa_e}{2}(x^2+y^2)}. \quad (6)$$

The degeneracy of the two-dimensional harmonic oscillator is

$$g_n = n + 1, \quad n \in \mathbb{N}_0. \quad (7)$$

According to the selection rules, which we get from the transition matrix element

$$M_{if} = \langle \psi_f | \mu | \psi_i \rangle, \quad (8)$$

where μ is the dipole operator, $|\psi_i\rangle$ the initial state and $|\psi_f\rangle$ the final state. Hence the transition from an electron state to a hole state is only allowed for the same quantum numbers n , i.e. $n_x = n_y$. Corresponding to the well known solutions of the hydrogen atom, we can identify different orbitals of the quantum dots, viz. the s , p , d , \dots -orbitals with quantum numbers $n = 1, 2, 3, \dots$. The analogy to atoms also arises from the similar structure of the energy levels. Hence the wave function with $n_x = n_y = 0$ (ground state) is called s -orbital. For better illustration the allowed transitions are depicted in figure 1.

If we use light with an energy higher than the band gap, we create electrons in the conduction band and holes in the valence band. Bound by the Coulomb-attraction a

electron-hole pair can form a quasiparticle known as *exciton*. Henceforth we just deal with excitons out of excited electrons and heavy holes, so called heavy-hole-excitons with spin ± 1 because they recombine by radiation. Due to phonon scattering, the exciton relaxes into the ground state. Indeed, it is also possible that a electron-hole-pair creates an exciton after or while relaxing into the ground state. If the electron then recombines with the hole, energy in form of a photon is emitted. This process is called the *photoluminescence* [4]. It is also possible that two excitons in the s -state of a quantum dot creates a biexciton with a slightly different energy than the exciton-energy. Figure 1 is also a good approximation for a quantum well, in which the depicted transition, i.e., an interband transition is allowed. Other possible transitions are excitonic or intersubband transitions.

Well Potential Model: Note that instead of a two dimensional oscillator-model of a quantum dot, it is also common to use a simple well potential with finite depth as mentioned above. A short calculation leads to two transcendental equations. They read

$$\tan \theta = \sqrt{\frac{\theta_0^2}{\theta^2} - 1}, \quad (9)$$

$$-\cot \theta = \sqrt{\frac{\theta_0^2}{\theta^2} - 1}, \quad (10)$$

where $\theta = ka/2$ has to be determined and $\theta_0 = mAa^2/2\hbar^2$ is a constant, depending on the mass of the particle m , the width of the potential well a , and A the depth of the well. Here k is the wave vector. The energy spectrum is then given by

$$E_k = \frac{\hbar^2}{2m} k^2. \quad (11)$$

Expectation for the Spectra: In this paragraph we try to explain the measured spectra and discuss their expected peaks. As we discussed in the case of the two dimensional harmonic oscillator each allowed transition in a quantum dot (see figure 1) will be imprinted in the spectrum. Considering the Pauli exclusion principle for the allowed occupancy of the degenerated states, each peak corresponding to an orbital will have different heights. Hence energy levels with a higher degeneracy g_n have higher peaks, so the peak of the s -orbital will be the smallest. Note, that due to the laser intensity not all peaks are visible, i.e., for low laser intensities only the lowest levels can be occupied and contribute to the spectra. Therefore, from high laser intensities will arise more peaks in the spectra of quantum dots. Moreover the peak of the substrate, e.g. GaAs ($\lambda = 1.519$ eV) will be imprinted in the spectrum [4]. By comparing the measured peaks with known substrate band gaps it is possible to identify the substrate's peak. Another contribution in form of a peak results from the quantum well as discussed above. To identify this contribution we can change the

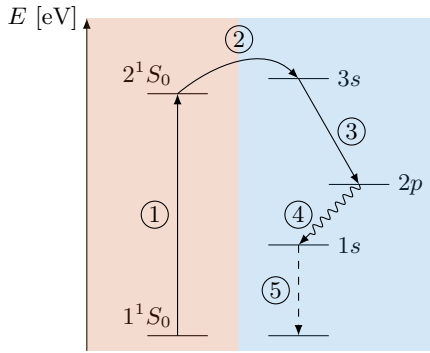


FIG. 2. Schematic scheme of a HeNe Laser. The states that corresponds to Helium are coloured in orange and the states for Neon are coloured in blue.

laser intensity and compare the height of the peaks. Likewise, the change of temperature will affect the measured spectrum. While we assumed low temperatures for the previous discussion we now change the temperature. Assume that we start at low temperature and all discussed peaks are visible. Increasing the temperature will lead to a vanishing of peaks due to the thermal fluctuations.

Experimental Methods

HeNe-Laser: In principle we can describe the HeNe-Laser as a four level system, where we use the Helium to pump the laser. The first level ① is the excitation from the ground state to the 2^1S_0 state of Helium via electron collisions. The second process ② are the collisions between Helium and Neon atoms where the $3s$ state of Neon is excited and populated. In the third step ③ the laser light of $\lambda = 632.8 \text{ nm}$ is emitted. Depending on the dispersive medium it is also possible to select other wavelengths. The system is then in the $2p$ state of Neon. The fourth level ④ is in this example the $1s$ state of Neon which we reach after a spontaneous decay from the $2p$ state. With further collisions ⑤ between the Neon atoms and the confining wall of the glass capillary tube the system will end in the ground state again. For better visibility the whole process is depicted in figure 2 [5].

Spectrometer: An optical spectrometer consists of an entrance slit, where light is guided through, curved mirrors or collimators, and a grating. Hence the light is diffracted at the grating and guided to a charge-coupled device (CCD). Therefore it is possible to extract the spectral information from the spatial separation. An spectrometer can also be used as a monochromator.

Monochromator: It is a device that allows to select the desired wavelength of light from a wider range of wavelengths. Typically a light beam is guided to an entrance slit of the monochromator. The slit is placed at the focus of a curved mirror or a collimator, respectively.

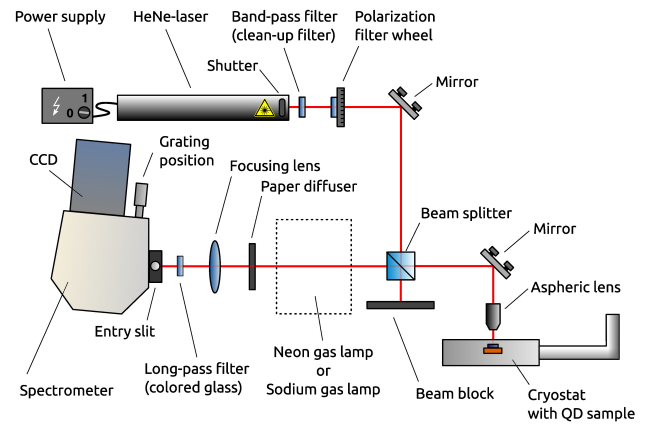


FIG. 3. Setup of the whole experiment. From [6].

The collimated light is then diffracted from a grating to another mirror where the light is refocused on an exit slit. Note that the grating is rotatable and so only the desired wavelength is focused on the exit slit.

We should stress, that in this experiment the spectra of the quantum dots are measured with the CCD inside the spectrometer.

Resolution: If we are dealing with spectrometers or monochromators, Rayleigh's criterion, which imposes a condition to the distance between two light sources or objects, plays a crucial role. According to Rayleigh's criterion it is possible to distinguish between two objects if the main maximum of diffraction belonging to one object is diffracted onto the first minimum of diffraction of the other object. In this context the resolution is the ability of an imaging device to separate points of an object at a small distance. In the case of diffraction at a circular aperture the angular resolution is given by

$$\theta = \frac{1.22\lambda}{D},$$

where θ is the angular resolution, λ the wavelength of the light, and D the diameter of the lens' aperture. The factor 1.22 is derived from a calculation of the position of the first dark circular ring surrounding the central Airy disc.

Using the Rayleigh criterion by inserting the minima, we can observe from the corresponding intensity profile, into the demand for constructive interference allows us to calculate the dispersion and hence deduce an equation for the spectral resolution A

$$mN = \frac{\lambda}{\Delta\lambda} \equiv A, \quad (12)$$

where $\Delta\lambda$ is the smallest wavelength difference we can distinguish at a given wavelength λ , m the order of diffraction, and N the number of grooves. According to IUPAC the resolution in optical spectroscopy is defined as the

wavelength divided by the minimal wavelength difference between two lines in the spectrum that can be distinguished.

Line broadening and shift: There are several reasons for line broadening and line shift of the spectra. The first is the broadening due to the *uncertainty principle*, which says that the lifetime of an excited state is related to the uncertainty of its energy. Hence a short life time results in a large energy uncertainty and in an unshifted Lorentzian profile. Another broadening which arises as a Gaussian profile is the *thermal doppler broadening*. Depending on the temperature the thermal fluctuations change and emitted photons are red- or blue-shifted. Obviously both effects occur in the measured spectra. In the case of quantum dots an additional broadening will appear in the spectra. Because in this experiment we will excite and detect several quantum dots instead of just one, the peaks in the spectrum will additionally be broadened in a Gaussian manner. This is due to the fact that each quantum dot grows to a different size, so the measured spectra are broadened. Because this line broadening dominates all others we will fit the spectra with numerous Gaussians as explained later. As we will see in the temperature series an additional *thermal red shift* arises in the spectra. For increasing temperature the lattice of the substrate, and the quantum dots as well as the corresponded tensions will extend and slightly change the band gaps.

ANALYSIS

In the following section we want to explain the experimental procedure, the experimental setup, and the analysis of the measured data. The used setup is depicted in figure 3. In this experiment we use two different types of quantum dots, namely InAs/GaAs and InP/InGaP, where the first part denotes the quantum dot and the second part the substrate. For more details see [6].

Experimental Procedure

The experimental procedure is divided into two days. Whereas the first day mainly concentrates on the calibration and resolution of the spectrometer, the second part contains the measurement of the spectra of the used quantum dots for different laser intensities and temperatures.

First Part

Calibration: Depending on the rotation of the grating in the spectrometer we can decide if light with the desired wavelength shines on the CCD camera. To calibrate the spectrometer we use a calibration lamp, i.e. a Neon-vapor lamp. The lamp has to be adjusted at the optical axis

TABLE I. Intensity of the laser as function of the angle of the polar filter.

Polar filter [°]	Intensity [mW]
10	0.0
20	0.15
30	0.69
40	1.33
50	1.89
60	2.38
70	2.65
80	2.7
90	2.65

in front of the entrance slit of the spectrometer. Note that the entrance slit is closed (0 μm). With a micrometre screw the central wavelength of the Neon spectrum is adjusted. With a peak of the well known Neon spectrum we can find the correct adjustments for the spectrometer software. This allows us to compare the recorded Neon spectra with the listed Neon emission lines to improve the adjustment of the spectrometer software.

Resolution: To determine the resolution of the spectrometer we centre a Sodium-vapor lamp on the optical axis in front of the entrance slit. Then the central wavelength of 589 μm is adjusted with the micrometre screw. Subsequently the Sodium doublet at 588.9558 nm and 589.5924 nm should be recorded for at least 10 different sizes of the entrance slit.

Second Part

Before we can record the spectra of the quantum dots we had to cool them down to 4 K. Additionally the optical elements, e.g. mirrors had to be adjusted. Note that there should be no unwanted reflexes in the whole setup. After that we can proceed with the cooled quantum dots. The subsequent steps are done for both types of quantum dots.

Power Series: At first the central wavelength is adjusted on the micrometer screw. A coloured density filter is used to suppress the laser light. Then for at least ten different laser intensities the spectrum of the quantum dots is measured. During all measurements the temperature should be at 4 K. The laser intensity is adjusted with a polarisation filter. In table I there are given the intensities belonging to different angles of the polar filter.

Temperature Series: The spectra of the quantum dots are measured at different temperatures. Therefore we use a heater. Starting from 10 K the temperature is increased in steps of 20 K till the spectrum becomes too noisy, typically at 150 K.

After finishing all measurements the experimental setup is shut down as described in the instructions.

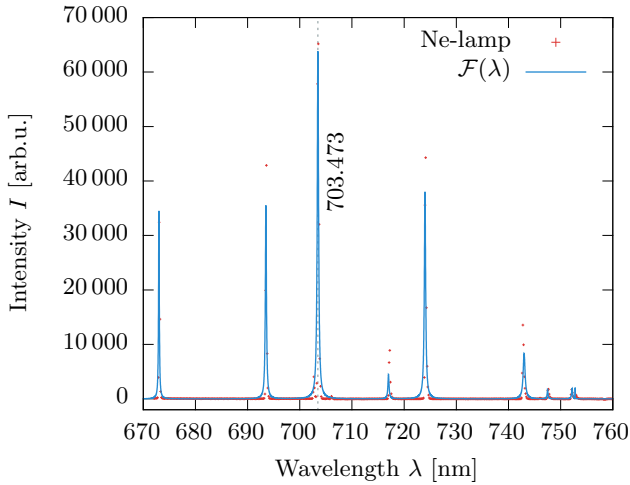


FIG. 4. Emission spectrum of the Neon vapour lamp. A vast multitude of sharp peaks is observable. The fitted function $\mathcal{F}(\lambda)$ is composed of numerous Gaussians.

Calibration

Due to the discussed types of broadening the spectra have the form of a Gaussian. As we are dealing with multiple peaks in most cases we certainly want to fit a sum of Gaussians to our data. We use a sum of N peaks of the form

$$\mathcal{F}(\lambda) = \sum_{i=1}^N a_i \cdot e^{-\frac{(\lambda - \mu_i)^2}{2\sigma_i^2}} \quad (13)$$

where the free parameters of the fit are the amplitude a_i , the central wavelength μ_i and the width σ_i of the single Gaussians.

Neon-vapour lamp: To calibrate the whole set up we use the well known spectrum of Neon. For our adjustment we concentrate on the most powerful peak which we could obtain in the measured spectra, viz. 703.4 nm. The measured emission spectrum of the neon vapour lamp is depicted in figure 4. For better visualisation the spectrum is fitted with equation (13). The highest peak corresponds to the wavelength 703.4 nm.

Resolution

Because the resolution of the spectrometer depends crucially on the size of the entrance slit, we use the well known spectrum of a sodium lamp to calculate the resolution. Therefore we increase the size of the entrance slit σ till the sodium D-lines are not visible anymore. The positions of the sodium D-lines are according to [7]

$$\begin{aligned} \lambda_{D_1} &= 589.755\,814\,7(15) \text{ nm}, \\ \lambda_{D_2} &= 589.158\,326\,4(15) \text{ nm}. \end{aligned} \quad (14)$$

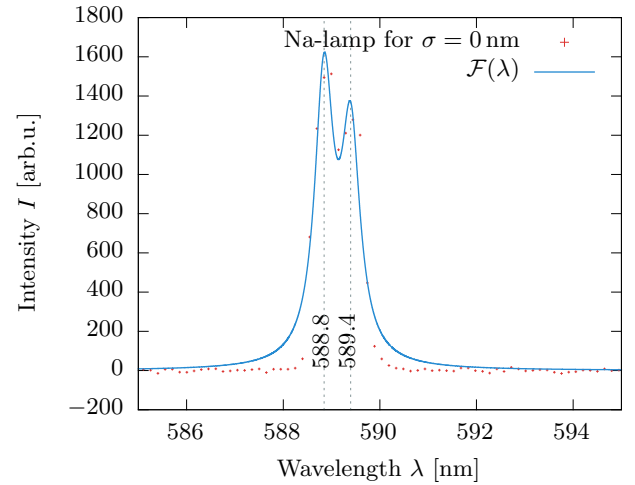


FIG. 5. The Na doublet for a slit width of $\sigma = 0 \mu\text{m}$.

As depicted in figure 5 for the right choice of the entrance slit (here the slit width is $\sigma = 0$) the sodium doublet arises. Due to our calibration the found doublet lines are at

$$\begin{aligned} \lambda_{D_1} &= 588.8 \text{ nm}, \\ \lambda_{D_2} &= 589.4 \text{ nm}. \end{aligned} \quad (15)$$

Note that, the experimental slit width $\sigma = 0$ does not mean that the entrance slit is totally closed. Within the precision of the micrometer screw it is closed. Compared to the literature values the D-lines are slightly shifted to smaller wavelengths. This is not really astonishing because as depicted in figure 6 for different slit widths the whole doublet starts wandering. From the figure we can see that for increasing slit widths the doublet wanders to higher wavelengths till we can only observe just one big peak, i.e., it is not possible to observe the sodium doublet for big slit widths. The shift to higher wavelengths originates from the fact that we could not adjust the lamp directly in front of the slit. Consequently, for increasing slit widths more and more bad adjusted light beams will enter the spectrometer and diffracted on the CCD to higher wavelengths. Nevertheless, it is possible to calculate the resolution of the spectrometer. According to the definition (12) we have to find the smallest distance between two lines, we can distinguish. This is at $\sigma = 350 \mu\text{m}$ the case. For bigger slit width we have only one peak. Hence the smallest wavelength difference is

$$\begin{aligned} \Delta\lambda &= \lambda_{\text{peak},1} - \lambda_{\text{peak},2} \\ &= 590.842 \text{ nm} - 589.352 \text{ nm} \\ &= 0.4 \text{ nm}. \end{aligned} \quad (16)$$

The resolution of the spectrometer is then given by

$$A = \frac{\lambda}{\Delta\lambda} = 1475.8,$$

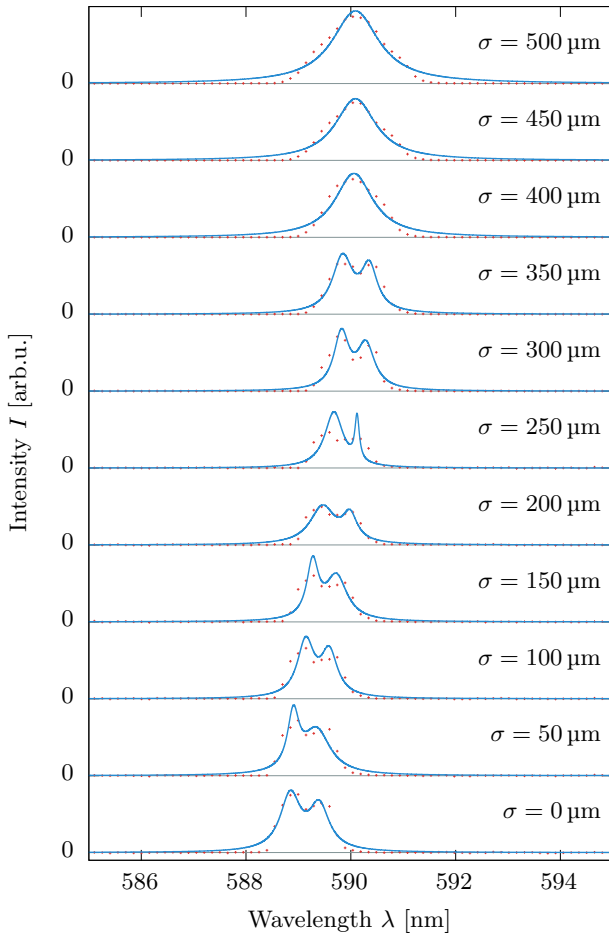


FIG. 6. The Na doublet vanishes for increasing width of the slit.

where we used the peak wavelength λ .

This also corresponds with Rayleigh's criterion which says, that it is only possible to distinguish two light sources if the main maximum of diffraction belonging to one light source (one of the peaks) is diffracted onto the first minimum of diffraction of the other light source (other peak). For bigger slit widths this criterion is not fulfilled anymore, so it is not possible to observe both D-lines. Note that sodium D-lines are the result of the fine structure splitting of the $3p$ -level of sodium, i.e., due to the coupling of electron spin with the orbital spin the $2p$ -level gives rise to two states with total momentum $j = 1/2$ and $j = 3/2$ [5].

Power Series

InAs/GaAs: In the spectrum of the InAs/GaAs quantum dots we expect a couple of peaks belonging to different kind of contributions, viz. from the quantum well, the substrate (GaAs), and the quantum dots themselves (see

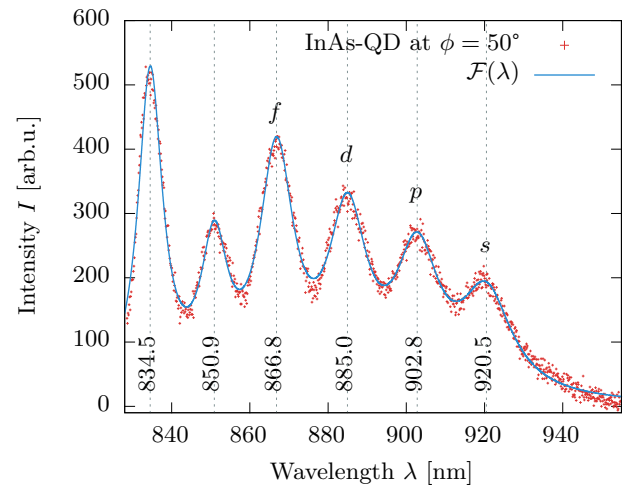


FIG. 7. Spectrum for InAs with fit of multiple Gaussian functions $\mathcal{F}(\lambda)$ at $T = 4$ K.

basics). The peaks corresponding to the orbitals will appear with different heights. Due to the degree of degeneracy (see basics) we expect higher peaks for higher orbitals. Obviously, we assumed that the chosen laser intensity is high enough to saturate all orbitals. The measured spectra of the InAs/GaAs quantum dots are depicted in figure 7. As shown all peaks, i.e., orbitals were visible at the laser intensity belonging to the polarisation filter angle 50° and the temperature 4 K. According to our choice of the central wavelength the emission wavelength of the orbitals are

$$\lambda_s = 920.5 \text{ nm}, \quad (17)$$

$$\lambda_p = 902.8 \text{ nm}, \quad (18)$$

$$\lambda_d = 885.0 \text{ nm}, \quad (19)$$

$$\lambda_f = 866.8 \text{ nm}. \quad (20)$$

The other two peaks corresponds to the quantum well and the GaAs substrate

$$\lambda_{\text{qw}} = 850.9 \text{ nm}, \quad (21)$$

$$\lambda_{\text{GaAs}} = 834.5 \text{ nm}. \quad (22)$$

The peak corresponding to the substrate can be identified by comparing with the known band gap of GaAs of 1.519 eV which is about 820 nm [4]. In figure 8 there are depicted the power series for the InAs quantum dots. Note that the angle ϕ corresponds to the adjustment of the polar filter which regulates the laser intensity. Here $\phi = 0^\circ$ means that we deal with a nearly vanishing laser intensity, and $\phi = 50^\circ$ we use the full laser power. As depicted the InAs/GaAs spectrum becomes more visible for higher laser intensities, so we can observe more orbitals. This also correspond with the theoretical concept because the higher the laser intensity the more electrons we can excite. We should also stress that at some point

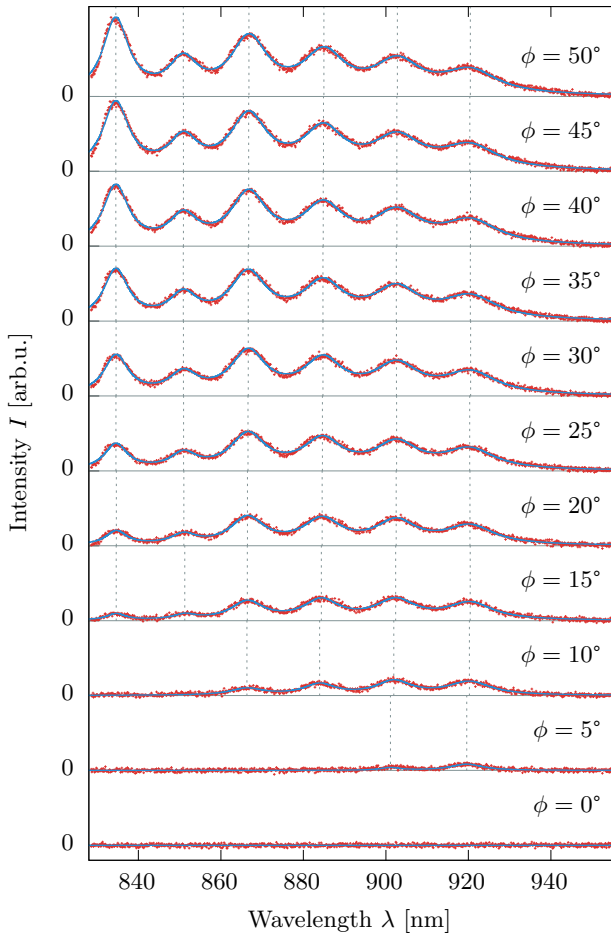


FIG. 8. Power series for the InAs/GaAs quantum dot at $T = 4$ K.

the spectrum saturates. Hence increasing the laser power is not necessary.

InP/InGaP: In this case we also expect the same contributions as described above. The spectrum of the InP/InGaP quantum dots is depicted in figure 9. As shown all peaks, i.e., orbitals were visible at the laser intensity corresponding to the polarisation filter angle 50° and the temperature 4 K. With the fit function (13) it is possible to find the wavelength of the peaks, i.e., the orbitals

$$\lambda_s = 751.5 \text{ nm.} \quad (23)$$

As we can see there is only one orbital, viz. the s -orbital. The big peak at 812.2 nm seems to belong to the quantum well or the substrate. The bandgap energy of InGaP is between the bandgap energy of GaP 2.338 eV (530 nm) and InP 1.421 eV (873 nm). If the exact ratio of Indium and Gallium is known it is possible to determine the exact bandgap energy (e.g. see [4]). Therefore the big peak seems to belong to the substrate. In figure 10 there is depicted the power series for the InP/InGaP quantum

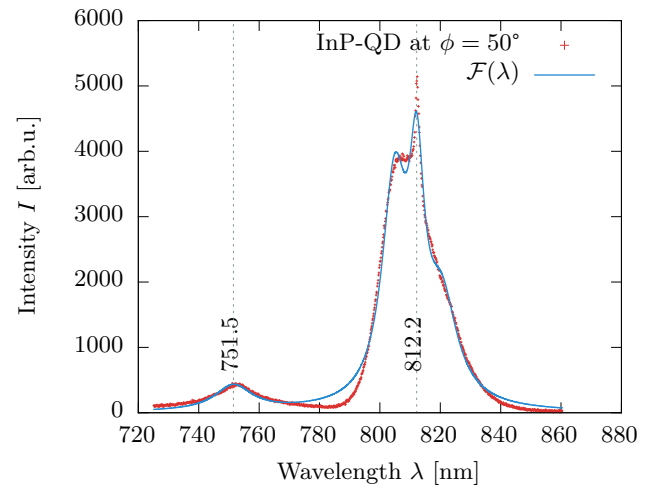


FIG. 9. Spectrum for InP/InGaP with fit of multiple Gaussian functions $\mathcal{F}(\lambda)$ at 4 K.

dots. The measurement process is exactly the same as in the case of InAs/GaAs, so are the labels of the figures. Again the InP/InGaP spectrum saturates for high laser intensities. Remarkably, for InP/InGaP this is already the case at $\phi = 10^\circ$. The explanation is, that in the case of InP/InGaP we deal with just one orbital. Hence it is possible to excite enough excitons already at low intensities. Note that, a higher intensity does not mean we can excite electrons at higher energy levels, it means that we can excite occupy more energy levels. In the case of the quantum dots we excite excitons or electrons which relax into the orbital states, so they can recombine and photoluminescence is possible.

Temperature Series

This section discusses the temperature dependence of the InAs/GaAs and InP/InGaP spectrum. We expect, that by increasing the temperatures more and more peaks in the spectrum will vanish and hidden by thermal fluctuations. For increasing temperature the number of phonons will increase, so the charge carriers can absorb phonons and a recombination is more likely than to reach a bound state in the quantum dots. Moreover the spectra will broaden and shifted due to the thermal doppler broadening and thermal red-shifting as discussed in the basics.

InAs/GaAs: The result of the temperature measurements of InAs is depicted in figure 11. The waterfall plot shows that it is impossible to observe spectra at higher temperatures, e.g., at 120 K. The cooler the quantum dots is, the less thermal fluctuations mask the spectrum.

InP/InGaP: The temperature measurement was repeated for InP. The results are depicted in the waterfall plot 12. The observations explained in the case of InAs/GaAs are also valid for InP/InGaP. The difference

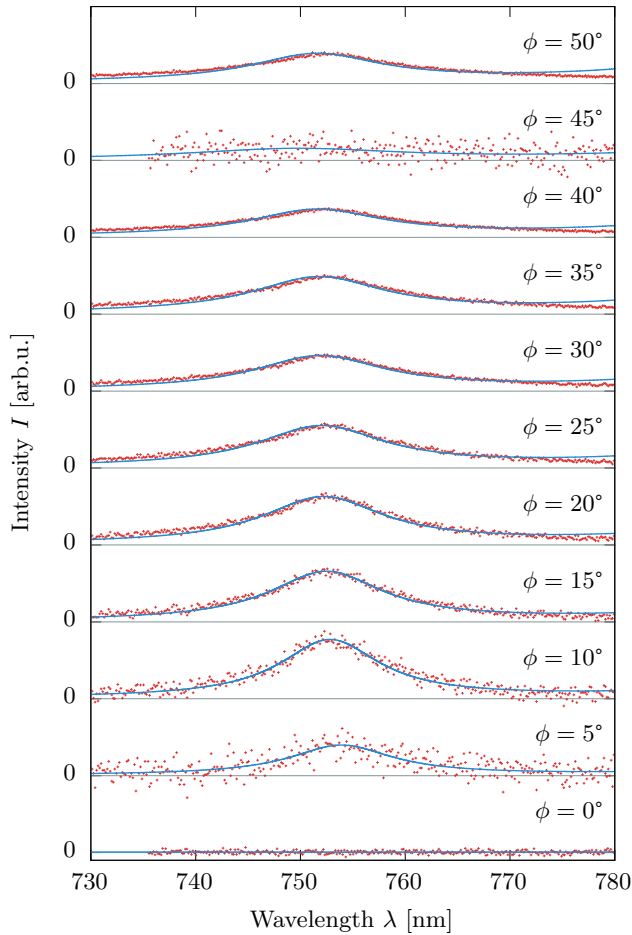


FIG. 10. Power series for the InP/InGaP quantum dot at $T = 4$ K. As shown at $\phi = 45^\circ$ there is no s -orbital visible. This is caused by a defective measurement.

between InAs and InP is the non-vanishing spectrum at higher temperatures. The spectrum of InP/InGaP is still visible at higher temperatures compared to the spectrum of InAs/GaAs.

We want to conclude this section by drawing a short recapitulation. Both measurements of the temperature series show that low temperatures are inevitable for measuring the spectra of quantum dots. Otherwise, thermal fluctuations mask the spectra. Moreover, the s -orbital of the quantum dots is the last vanishing peak at high temperatures. This might be due to the degeneracy of each orbital. So the temperature dependence was consistent with the predicted expectations.

SUMMARY

The whole experiment is mainly divided in two experimental tasks.

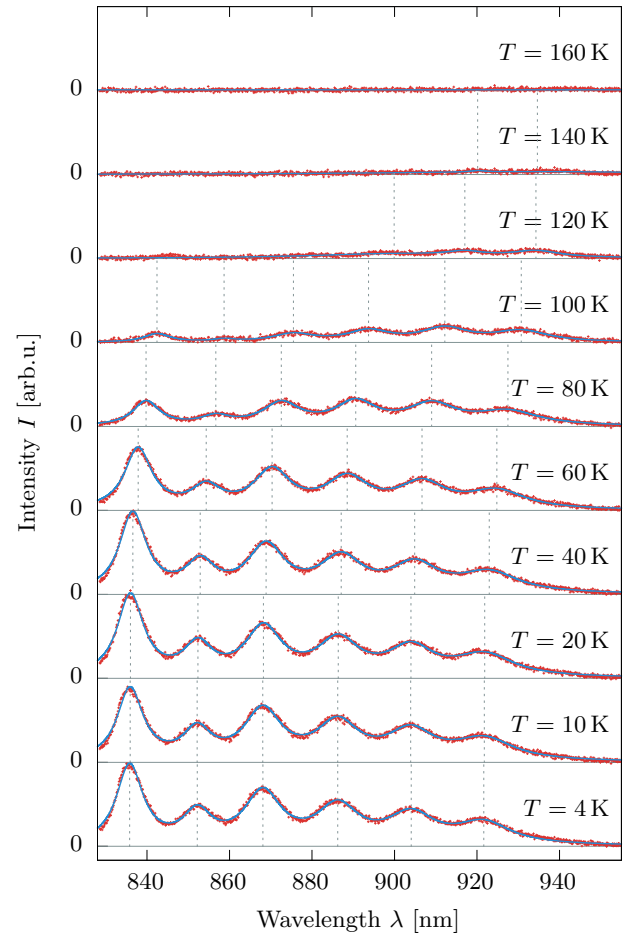


FIG. 11. Temperature series for the InAs/GaAs quantum dot at $\phi = 50^\circ$.

First part: In the first part the experimental setup was calibrated with the help of the well known spectrum of a Neon vapour lamp, so we could adjust the software of the spectrometer at the 703.4 nm peak. With help of the sodium lamp the dependency of the resolution on the slit width was investigated. Hence the double lines were only visible for small slit widths, which corresponds with Rayleigh's criterion. Varying the slit width allows to determine the resolution of the spectrometer. From our measurements we found a resolution of

$$A = 1475.8, \quad (24)$$

by a peak to peak distance of

$$\Delta\lambda = 0.4 \text{ nm}. \quad (25)$$

Second part: In this part we investigated the spectra of different types of quantum dots for different laser intensities and temperatures. In the case of InAs/GaAs, all orbitals were visible for higher laser intensities and low temperatures. Additionally, all visible peaks have

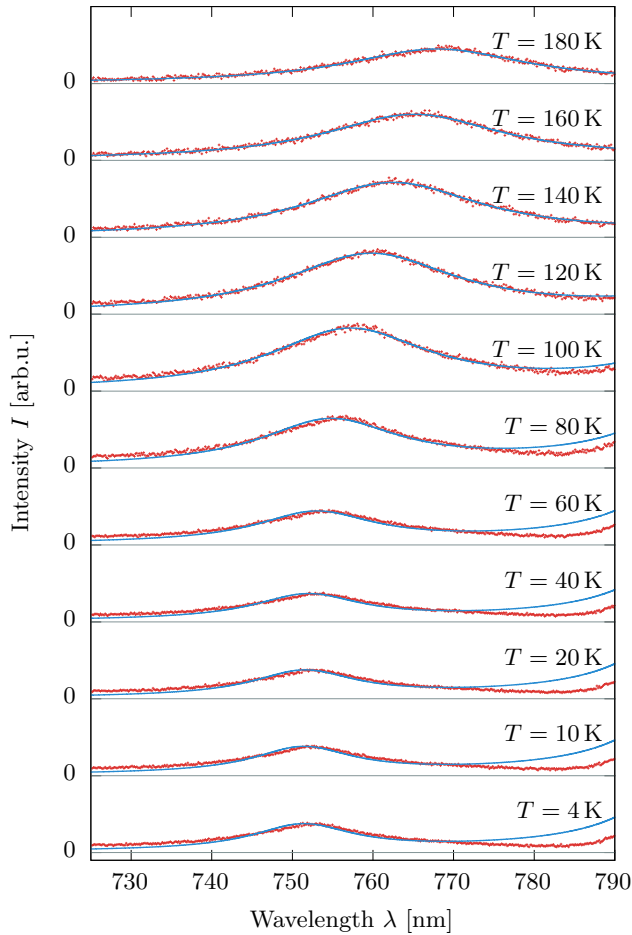


FIG. 12. Temperature series for the InP/InGaP quantum dot at $\phi = 50^\circ$.

nearly an equidistant distance, which agrees with the two dimensional oscillator-model presented in the basics. Due to thermal fluctuations it was not possible to observe the spectrum at temperatures higher than 120 K. However, in the case of InP/InGaP the spectrum was also visible at temperatures up to 140 K. Nevertheless, both quantum dots showed the same behaviour. For low laser intensities and high temperatures an observation of the spectra is impossible. Note that due to thermal doppler broadening and the uncertainty principle the spectra are broadened and slightly shifted by varying the temperature and due to the fact that we excite an ensemble of quantum dots.

* Michael_1233@gmx.de

† henrimenke@gmail.com

[1] P. Michler, *Fortgeschrittene Festkörperphysik* (2014).

[2] D. Bimberg, M. Grundmann, and N. N. Ledentsov, *Quantum dot heterostructures* (John Wiley & Sons, 1999).

- [3] U. Seifert, *Theoretische Physik 2*, 1st ed. (Universität Stuttgart, 2013).
- [4] S. Hunklinger, *Festkörperphysik* (Oldenbourg Wissenschaftsverlag, 2007).
- [5] H. Haken and H. C. Wolf, *Atom- und Quantenphysik: Einführung in die experimentellen und theoretischen Grundlagen* (Springer-Verlag, 2013).
- [6] M. Mustermann, *Photolumineszenz von Quantenpunkten* (2015).
- [7] P. Juncar, J. Pinard, J. Hamon, and A. Chartier, *Metrologia* **17**, 77 (1981).